ANTIOXIDANTS & REDOX SIGNALING
Volume 13, Number 6, 2010

DOI: 10.1089/ars.2009.2977

ORIGINAL RESEARCH COMMUNICATION

Neuroglobin Overexpression in Cultured Human Neuronal Cells Protects Against Hydrogen Peroxide Insult *via* Activating Phosphoinositide-3 Kinase and Opening the Mitochondrial K_{ATP} Channel

Shane T. Antao,[1,2] T.T. Hong Duong,[1,2] Roshanak Aran,[1] and Paul K. Witting[1,2]

Abstract

Cultured neurons tolerate low H_2O_2 concentrations ($\leq 50\,\mu M$) through the activity of constitutive antioxidant response elements (ARE). At H_2O_2 levels ($\geq 100\,\mu M$), neurons increase expression of the gene encoding for inducible hemoxygenase-1 while superoxide dismutase-2 and catalase remain unchanged. Despite this adaptive response, the endogenous antioxidant systems are overwhelmed, leading to decreased viability. Elevating the neuronal cell content of human neuroglobin (Ngb) prior to insult with 100 or $200\,\mu M$ H_2O_2 enhanced cell viability and this resulted in a significant decrease in oxidative stress and an increase in the intracellular ATP concentration, whereas in parental cells exposed to the same H_2O_2-insult, oxidative stress and ATP increased and decreased, respectively. The mechanism for this increase in ATP involves sustained activation of the mito-K_{ATP} channel and an increase in phosphoinositide-3 kinase (PI3K)-mediated phosphorylation of Akt. Pharmacological inhibitors directed toward PI3K (wortmannin and LY294002), or the mito-K_{ATP} channel (glybenclamide) inhibited the H_2O_2-mediated increase in ATP in cells overexpressing human Ngb and consequently cell viability decreased. Neuroglobin's ability to bolster the intracellular pool of ATP in response to added H_2O_2 is central to the preservation of cytoskeletal integrity and cell viability. *Antioxid. Redox Signal.* 13, 769–781.

Introduction

The high mortality and morbidity resulting from stroke (48) has focused research towards understanding the cerebral response to ischemia with one main goal: to identify molecular targets suitable for development as potential therapies. However, for the most part neuroprotective agents identified in preclinical studies have been disappointing in human trials (21, 65).

Neuroglobin (Ngb) is a heme-protein from the globin superfamily and is expressed in the brain (62), central nervous system, and retina (16). To date, the exact function of Ngb has yet to be elucidated, but there are several proposed mechanisms. Similar to hemoglobin (Hb) and myoglobin (Mb), Ngb reversibly binds oxygen (10) and may participate in oxygen transport, storage, and release. This may involve formation of a disulfide bond within the protein backbone that introduces subtle changes to the distal cavity region (21). Despite this knowledge, the biological function of Ngb remains unclear. Previous studies have implicated Ngb to be involved in scavenging reactive oxygen species (ROS) (24), modulating nitric oxide ($^{\bullet}NO$) (19) and intracellular metal ion homeostasis (13), and/or serving as an oxygen sensor (9, 56).

Changes in Ngb expression correspond to the severity of histological and functional deficits after stroke (52). However, questions remain as to whether neuroprotection is conferred by Ngb (27). Enhanced Ngb expression is linked to neuroprotection in some (51, 52) though not all models of ischemic stroke (43). This conflict in the available literature indicates further studies are required to establish whether Ngb can protect neurons from ischemic insult, and if so, the mechanism(s) involved in this biological activity.

The loss in blood supply to oxygen-sensitive brain tissue leads to cerebral oxidative stress (2). Enhanced oxidative stress promotes production of oxidants, including superoxide radical anion ($O_2^{\bullet -}$) and its dismutation product hydrogen peroxide (H_2O_2) (24)— both promote brain injury following stroke (36). The abundance of mitochondria in the ischemic brain are a major source of oxygen-centered radicals, and induction of mitochondria dysfunction leads to overproduction

[1]Redox Biology Group, Discipline of Pathology, Bosch Institute, Faculty of Medicine, The University of Sydney, Sydney, Australia.
[2]Vascular Biology Group, The ANZAC Research Institute, Concord Hospital, Concord, Sydney, Australia.

of $O_2^{\bullet -}$ with parallel increases in H_2O_2 within the affected cerebral tissue (50). For example, experimental forebrain ischemia reperfusion yields [H_2O_2] up to 100 μM in the rat brain (28).

Scavenging of ROS has been identified as one mechanism of action for Ngb in cultured human neuronal cells overexpressing the hemoprotein (17, 34). We also identified alternate secondary mechanisms that contribute to its protective activity in response to experimental ischemia (13), including maintenance of intracellular metal ion homeostasis and cytoskeletal integrity. Herein, we expand on our initial observations and determine whether Ngb's activity extends to protecting neuronal cells challenged with H_2O_2 as a model for free radical formation in the brain after ischemic insult.

Materials and Methods

Cell culture materials and general chemicals were from Sigma-Aldrich (Sydney, Australia) and were the highest quality available. Buffers were prepared in MilliQ water.

Human Ngb construct

Cloning of the Ngb open reading frame was performed with recombination-based Gateway technology (Invitrogen, Sydney, Australia), as described elsewhere (13). The construct containing the (hexa-HIS and V5) flanking peptides was confirmed using BigDye Terminator Cycle Sequencing (SUPAMAC, Sydney, Australia) and was used in all cell manipulations.

Cell transfection

The human Ngb plasmid DNA was transfected into the neuroblastoma cell line SH-SY5Y using Lipofectamine 2000 (Invitrogen). Transfection was achieved with high efficiency (~90%–95%), as described previously (13). Cells transfected with the PDEST40 blank vector yielded the parental (control) cells. Accumulation of the human Ngb-fusion protein in differentiated cells was verified by Western blot analysis with an antibody raised against a V5-epitope (Supplemental Fig. 1A; see www.liebertonline.com/ars). Concentration of the Ngb-fusion protein was estimated with densitometry by comparison to a standard curve. A commercial source for human Ngb was unavailable so equine Mb was used as standard and detected using a human Mb antibody that cross-reacted with the horse protein (Supplemental Fig. 1B; see www.liebertonline.com/ars). Overall, the concentration of the Ngb-fusion protein was ~13 μg/200 μl-cell lysate corresponding to 3.7 μM, which is approximately 4-fold greater than that estimated in the brain (62). The cell content of human Ngb-fusion protein was unaffected by treatment with H_2O_2 2 h after insult, implying that H_2O_2 did not modulate Ngb-fusion gene expression (Supplemental Fig. 1A).

Cell culture

The neuroblastoma cell line SH-SY5Y transfected with the blank vector (referred to hereafter as parental cells) or with human Ngb (Ngb-transfected cells) were inoculated at a density of ~1×10^4 cells and subcultured in Dulbecco's Modified Eagle's Medium/Ham's F12 (JRH Biosciences, KA) containing 10% fetal bovine serum, 100 units/ml penicillin, 100 μg/ml streptomycin, 2.5 mM L-glutamine, and 5 ml of nonessential amino acid solution, at 37°C in an atmosphere of 5% $CO_{2(g)}$. Studies were performed with cells grown to ~70%–80% confluence yielding ~5×10^6 to ~5×10^9 cells/ml.

Cells were induced to differentiate into a neuronal phenotype by treatment with 50 ng/ml of 12-*o*-tetradecanoylphorbol-13-acetate (TPA) over a period of 3 days (exchanging media every day of subculture). The neuronal phenotype was verified by monitoring mRNA expression of the neuronal cell marker growth-associated protein (GAP-43) with quantitative RT-PCR (Supplemental Fig. 2; see www.liebertonline.com/ars) as described previously (13).

Cell model

Differentiated neurons were prepared for challenge with H_2O_2 by substituting growth media with HEPES-buffered physiological saline solution (HPSS) containing: 22 mM HEPES (pH 7.4), 124 mM NaCl, 5 mM KCl, 1 mM $MgCl_2$, 1.5 mM $CaCl_2$, 0.16 mM HPO_4, 0.4 mM H_2PO_4, 5 mM $NaHCO_3$, and 5.6 mM D-glucose. Next, vehicle (phosphate buffered saline; PBS, pH 7.4) or a bolus of H_2O_2 was added (10, 50, 100 to 200 μM) and the cells re-cultured at 37°C for 2 h. Cells were harvested by scraping and cell pellets were obtained by centrifugation (~56 *g*). In some cases, cell pellets were immediately frozen in liquid nitrogen and stored at −80°C for use in biochemical studies.

Flow cytometry

Cell viability. To determine oxidative stress response in neurons, cells were pretreated with 50 μg/ml nonfluorescent dihydrorhodamine (DHR-123), then exposed to H_2O_2 (0–200 μM). Oxidation of DHR-123 yields the fluorescent product R-123. Mean fluorescence intensity was used as a surrogate marker for oxidative stress and was measured by flow cytometry (FACSCalibur BD Biosciences, Sydney, Australia) with excitation (Ex) 488 nm and Emission (Em) 540 nm.

Similarly, apoptosis and necrosis was determined using flow cytometry with a commercial Annexin V-FITC detection kit (BD Biosciences). Binding of FITC-conjugated annexin V (Ex 488 nm; Em 520 nm) and the counterstain propidium iodide (PI) (Ex 488 nm; Em 620 nm) was analyzed as described previously (32). To assess the involvement of mito-K_{ATP} channels or phosphoinositide-3 kinase (PI3K), complementary studies were performed with parental cells incubated with a selective mito-K ATP channel opener (57) (diazoxide; 100 μM, 10 min, 37°C), or an activator of PI3K (23) (human leptin; 100 nM, 30 min, 37°C) then challenged with H_2O_2.

Ca^{2+} content. Cells were then challenged with H_2O_2 (0–200 μM) for 2 h, the HPSS replaced with Dulbecco's buffered phosphate saline (DBPS; deficient in Mg^{2+} and Ca^{2+}cations) and intracellular Ca^{2+} was assessed with flow cytometry (Ex 506 nm; Em 526 nm) as described previously (60). Esterified Fluo3AM enters cells where esterases yield the active intracellular Ca^{2+} probe. An advantage for this probe is that it is not necessary to monitor two emission wavelengths to determine Ca^{2+} flux. The possibility of unrestricted Ca^{2+} uptake during cell harvest was nullified by using DBPS deficient in multiply charged cations.

Caspase activation. The activity of effector or executor caspases-3 and -7 was measured using a commercial kit

(Caspase-Glo™ 3/7, Promega, Australia). Briefly, cells were treated with 0–200 μM H_2O_2 and incubated for 2 h. Growth supplement was replaced with PBS and Caspase-Glo™ 3/7 reagent added (1:1 v/v; 20°C for 40 min) and total caspase 3/7 activity assessed by measuring luminescence with a Victor III Multi-label plate reader (Perkin Elmer, Sydney, Australia). Data sets were analyzed and expressed as a fold-increase in activity relative to the controls.

Intracellular ATP and mitochondrial function. The ratio of intracellular ATP/ADP (Perkin Elmer) and the absolute levels of ATP (ATPlite®, Perkin Elmer) were determined with commercial kits (47). Neuronal cells were cultured in 96-well plates, treated with H_2O_2 (0–200 μM), incubated for 2 h and then the samples were analyzed with a Victor III Multi-label plate reader according to the manufacturers instructions. Cellular ATP was normalized against total cell protein to account for any differences in cell density. Cell protein was determined using the BCA assay (Sigma).

Mitochondrial depolarization (a surrogate for mitochondrial dysfunction) was determined by flow cytometry. All samples were incubated with 200 μM MitoProbe, JC-1© (Molecular Probes, Eugene, OR) for 20 min at 37°C. Cell suspensions were centrifuged, the pellet washed and resuspended in 500 μl PBS and then analyzed. Emissions monitored at 525 and 620 nm were used to determine the shift of green to red fluorescence expressed as a fold-change in mean fluorescence intensity compared to the control.

Total ATP was also assayed in cells pre-incubated with chemical mediators. Cells were pre-incubated with 10 μM glybenclamide, a mito-K_{ATP} channel inhibitor (3), 250 nM wortmannin or 50 μM LY294002, 2-(4-Morpholinyl)-8-phenyl-4H-1-benzopyran-4-one hydrochloride, as inhibitors of PI3K (42), for 20 min at 37°C prior to H_2O_2-insult. The wortmannin concentration employed was selected as specificity is lost at higher doses (49). Intracellular ATP was also assessed in parental cells treated separately with 100 μM diazoxide (10 min, 37°C) or 100 nM human leptin (30 min, 37°C), prior to H_2O_2 insult (2 h, 37°C).

Chromatographic determinations of ATP

Changes in ATP were verified using complementary HPLC measurements. After H_2O_2 treatment, both parental and Ngb-transfected cells were lysed with ice cold $NaClO_4$ (400 μM). The samples were centrifuged (3000 *g*, 5 min), the supernatant placed on ice and treated with ice cold 1 *M* $NaHCO_3$, centrifuged again (13,000 *g*, 3 min) and the supernatant was analyzed by reversed-phased (LC-18) HPLC with gradient elution. Solvents consisted of (A) 0.15 *M* $NH_4H_2PO_4$ (pH 6.0) and (B) a mixture of acetonitrile/methanol (1/1, v/v). Analysis was performed using a (1 ml/min) linear gradient from 100% A to 85% A and 15% B as described (61). The column was equilibrated with buffer A for 10 min before sampling continued. Cellular ATP was monitored at 260 nm and was quantified by peak area comparison. Authentic ATP (purity 99%) eluted at ~5 min. Intracellular ATP was expressed as fold-change relative to the control (assigned unitary value).

Gene and protein regulation

After exposure to 0–200 μM H_2O_2, cells were lysed and total RNA extracted with a Total RNA Kit (Sigma) as per manufacturer's instructions. Complementary cDNA was constructed by reverse transcriptase-polymerase chain reaction (RT-PCR) using BioScript Rnase H Minus (Bioline, Sydney, Australia) and an Eppendorf Master-Cycler. Reaction mixtures contained: 2 μl total RNA, 1 μl oligo (dT), and 9 μl diethyl-pyrocarbonate (DEPC) treated Nanopure water. Reactions were then heated (70°C, 5 min) and then chilled (4°C, 5 min). Mixtures were further treated with 1 μl RnaseOut (an RNAase inhibitor), 1 μl dNTP Mix (PCR Grade), 4 μl of 5× reaction buffer (supplied by the manufacturer), 1.75 μl DEPC-treated nanopure water, and 0.25 μl Bioscript Rnase H Minus (Bioline) to a total volume of 20 μl. All samples were heated to 42°C for 60 min and then to 70°C for 10 min to stop the reaction.

Gene-specific PCR amplification was carried out using Biomix Master Mix (Bioline, Sydney, Australia) with an Eppendorf Master-cycler system. Primer sets were synthesized by Proligo (Table 1). Cycling consisted of activation (94°C, 5 min), 45 cycles of denaturation (94°C, 30 s), annealing for 30 s, elongation (72°C, 1 min), and then another elongation step (72°C, 10 min). Amplified cDNA was resolved on 2% agarose containing 2 μg/ml ethidium bromide. Gels were imaged using a BioDocAnalyzer (Biometra, Gottingen, Germany) and transformed to TIF for manipulation with Microsoft Power Point (2000). Semiquantitative densitometry was performed with ImageJ v1.30 software (http://rsb.info.nih.gov/ij/; NIH, Bethesda, MD; accessed March 24, 2010) and data expressed as fold-change in *β-actin*-normalized expression.

Western blot analysis

Western blot studies were performed as described in detail elsewhere (39). For studies on the HO-1 protein, microsomal isolates (see below) were first adjusted for protein content prior to loading onto gels. After separation on SDS-PAGE, detection of HO-1 was achieved with a rabbit polyclonal antibody raised human HO-1 (final dilution 1:2000 v/v) and a goat anti-rabbit IgG-HRP conjugate (final dilution 1:10,000 v/v).

Table 1. Primer Sequences Used to Assess Antioxidant Gene Regulation

Gene	*Sense*	*Anti-sense*
β-actin	5′-GGACTTCGAGCAAGAGATGG-3′	5′-AGCACTGTGTTGGCGTACAG-3′
HO-1	5′-GAGATTGAGCGCAACAAGGA-3′	5′-AGCGGTAGAGCTGCTTGACT-3′
MnSOD	5′-CCACTGCAGGACCTCATTTT-3′	5′-CACCTTTGCCCAAGTCATCT-3′
CAT	5′-ACATGGTCTGGGACTTCTGG-3′	5′-CAAGTTTTTGATGCCCTGGT-3′

All primer sequences were designed using the Primer 3 sequencing program (available on the Internet). Sense and anti-sense primers were synthesized by Proligo (Lismore, NSW Australia). Annealing temperature was 60°C for all primers.

Detection of total Akt protein (and its phosphorylated form) was performed by Western blotting and subsequently validated with a Ser473-p-AKT/t-AKT dual label CELISA kit according to manufacturer's instructions (Millipore, Sydney Australia). Cell lysates were separated on SDS-PAGE, proteins transferred to nitrocellulose, and the blots assessed for total Akt (t-Akt) (dilution 1:1000 v/v) and phosphorylated Akt (Ser473-p-Akt) (dilution 1:1000 v/v) (~60 Kda) using appropriate antibodies (Cell Signalling Technology, Brisbane, Australia). As a positive control, shrimp alkaline phosphatase (SAP) (Quantum Scientific, Sydney, Australia) was used in parallel samples to dephosphorylate proteins before visualization with enhanced chemiluminescence detection (WESTZOL™ Biotech., Gyeonggi-do, Korea) (39). A loading control was performed on a parallel blot using a polyclonal anti-human β-actin (Sapphire Bioscience, Sydney, Australia). Images were captured (KODAK Imaging system) and converted to "tagged image files" for further manipulations with Microsoft Office 2007. Where required, CELISA plates were analyzed with a FLUOstar Multilabel plate reader (BMG Labtech, Sydney Australia) with fluorescence parameters: Akt–Ex 500 nm; Em 550 nm; p-Akt–Ex 360 nm; Em 460 nm.

Hemoxygenase activity. Total HO activity was assessed in microsomal preparations prepared as described elsewhere (47). Assays were performed using 400–600 μg microsomal protein. Total HO activity was determined by monitoring bilirubin (BR) formation (product of heme catabolism) with gradient reversed-phase HPLC (47). The detection limit for BR under these conditions was ~15 pmol with authentic BR eluting at ~8.5 min. Finally, activity was expressed as a fold-increase in BR compared to the corresponding control.

Assessment of cell structure and receptor-mediated transport

Immunostaining. Cells were grown onto coverslips in DMEM/HAM's F12 media, then differentiated for 3 days using TPA as described previously (13). Next, the media was replaced with HPSS containing H_2O_2 (concentrations indicated in the figure legends) and cells subcultured in 5% $CO_{2(g)}$ at 37°C. After 2 h, media was aspirated, cells were fixed in methanol, and blocked with 1% w/v BSA at 37°C. After 30 min, the blocking buffer was removed and primary antibody (see below) was added and incubated at 20°C. After 1 h, cells were washed (3×PBS), incubated with the secondary antibody for 1 h, and finally visualized.

Cytoskeletal structure. Staining of cytoskeletal β-actin was performed with a monoclonal antibody raised against human β-actin (dilution 1:100 v/v), along with an anti-mouse–FITC conjugate secondary antibody (dilution 1:2500 v/v) that was visualized with Ex 530 nm.

Receptor-mediated endocytosis. A fluorescently labeled transferrin isoform (conjugated to Alexa Fluor 488, Invitrogen) was employed to assess receptor-mediated endocytosis, both before and after exposure of neurons to H_2O_2 (range 0–200 μM). Cells were incubated in 50 μg/ml of labeled transferrin (10 min, 37°C) prior to H_2O_2 challenge. Next, excess transferrin was removed by thorough washing in 0.2 *M* acetic acid containing 0.5 *M* NaCl (pH 2.8; 10 min at 4°C). Cells were fixed by incubating in 4% w/v paraformaldehyde (pH 7.5; 15 min; 20°C) and visualized with an Axiovert 200 inverted fluorescent microscope. Images were false-colored subsequent to acquisition using AxioVision software (AxioVision v4.5, Carl Zeiss, Australia).

Statistical analyses

Analyses were performed with Prism Software (*v*3.0, GraphPad Software Inc). Data were analyzed using One-way ANOVA with Bonferroni's post-hoc analysis or by Student *t*-test using Welch's correction for unequal variances. Statistical significance was set at $p < 0.05$.

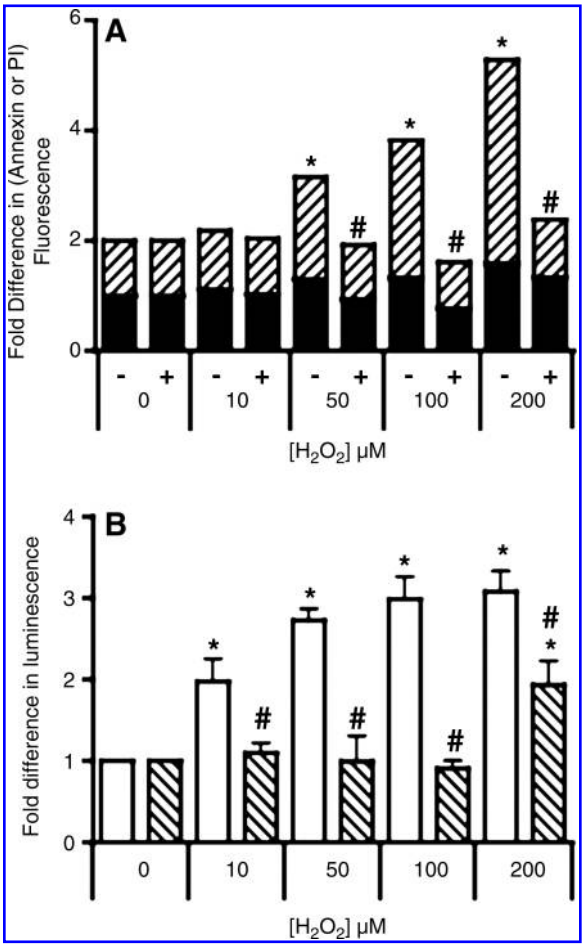

FIG. 1. Cell viability in differentiated parental (-) and Ngb-transfected (+) cells before and after exposure to H_2O_2. (**A**) Changes in apoptosis (*filled bar;* annexin stained) and necrosis (*hatched bar;* propidium iodide (PI) stained), respectively. Data represent means; $n = 3$ independent cell preparations. For simplicity, standard deviations (SD) are not shown (maximal SD was $\leq 12\%$). (**B**) Effector caspase3/7 activation in parental (*open bar*) and Ngb-transfected cells (*hatched bar*). Data represent mean ± SEM; $n = 3$ independent cell preparations. *Different to the control; $p < 0.05$. #Different to the parental cells at the corresponding H_2O_2 dose; $p < 0.05$. Caspase3/7 activity expressed as a fold-change relative to the vehicle-treated control arbitrarily assigned a value of 1.

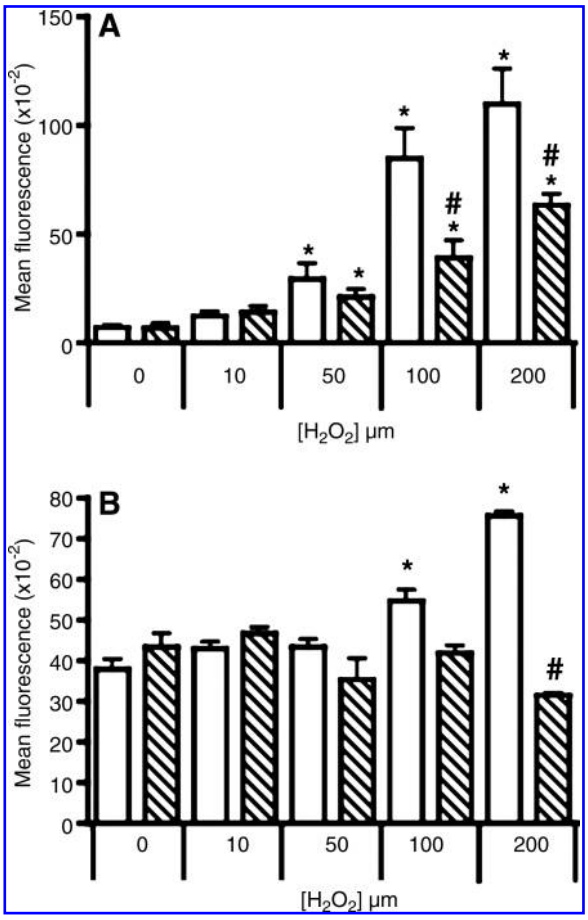

FIG. 2. H_2O_2-stimulated oxidative stress and mitochondrial dysfunction in parental and Ngb-transfected neurons. (**A**) Parental (*open bar*) and Ngb-transfected (*hatched bar*) cells were pre-loaded with 50 μg/ml dihydro-rhodamine and rhodamine fluorescence measured after exposure to H_2O_2 insult. Data represent mean ± SD; $n = 4$ independent duplicate studies. (**B**) Mitochondrial membrane depolarisation was determined in parental (*open bar*) or Ngb-transfected (*hatched bar*) cells at the H_2O_2 dose indicated by using flow cytometry. Data is represent mean ± SD; $n = 3$ independent duplicate experiments. *Different to the control in the absence of H_2O_2; $p < 0.05$. #Different to the parental cells at corresponding H_2O_2 dose; $p < 0.05$.

Results

Cell viability

Initial studies demonstrated that apoptosis increased significantly in parental cells when measured 24 h post-insult yet cells transfected with human Ngb were significantly protected from apoptosis at all H_2O_2 concentrations investigated (Supplemental Fig. 3; see www.liebertonline.com/ars). In contrast, cell viability measured 2 h post insult showed a marked absence of apoptosis in both cell types and this was judged as a useful time point to assess all molecular and biochemical response(s) to added H_2O_2 in the absence of any marked change in cell viability.

Exposure of cultured parental cells to 10 μM H_2O_2 for 2 h elicited no change in the extent of apoptosis and necrosis as compared to the vehicle-treated controls (Fig. 1A). This suggested that the endogenous neuronal antioxidant capacity was sufficient to cope with this level of insult. However, necrosis increased significantly and dose-dependently in parental cells exposed to 50–200 μM H_2O_2 for 2 h, reaching ~3-fold higher levels than the control. Under these conditions, the proportion of apoptotic cells remained unchanged. Cells overexpressing human Ngb showed comparable resistance to 10 μM H_2O_2 insult. However, when exposed to 50–200 μM H_2O_2 cells overexpressing human Ngb showed a continued tolerance to H_2O_2 insult with consistently lower levels of necrosis and no measurable change in apoptosis relative to controls.

Caspase activation

Activity of the effector caspases 3/7 increased signficantly in a H_2O_2 dose-dependent fashion in parental cells exposed to 50–200 μM H_2O_2 (Fig. 1B). Cells transfected with the human Ngb–fusion protein showed marked resistance to caspase activation with the extent of caspase activity only reaching significance at the highest H_2O_2 dose tested. Despite being unable to detect apoptosis 2 h after insult (as judged by annexin V staining), neuronal cells exposed to H_2O_2 (final concentrations ≥ 10 μM) showed increased effector 3/7 activation that was inhibited by the overexpression of human Ngb.

Oxidative stress in neuronal cells exposed to H_2O_2

Treating cultured neuronal cells with 0–200 μM H_2O_2 for 2 h resulted in a dose-dependent increase in R-123 fluorescence, reaching more than 15-fold greater than that in control cells treated with vehicle alone (Fig. 2A). Cells overexpressing human Ngb displayed significantly lower fluorescent intensity than the parental cells at all corresponding H_2O_2 doses.

Mitochondrial membrane potential

Parental and Ngb-transfected neuronal cells exhibited similar resistance to mitochondrial dysfunction induced by 10 or

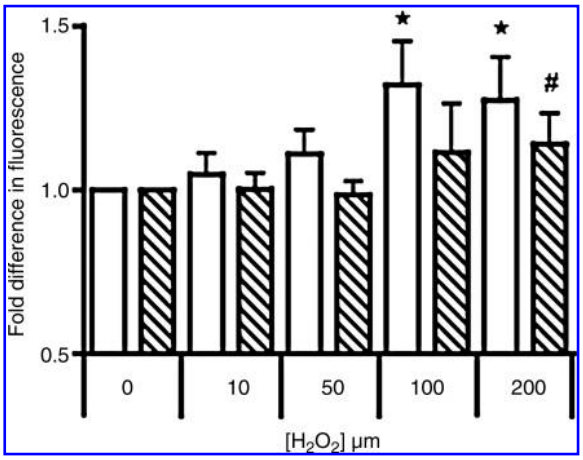

FIG. 3. Uptake and distribution of Ca^{2+} ions in parental cells is affected by increasing H_2O_2 challenge, whereas overexpression of human Ngb abrogates this influx. Cells were pre-loaded with Fluo3-AM and intracellular Ca^{2+} concentration was measured in parental (*open bar*) and Ngb-transfected cells (*hatched bar*) at the indicated H_2O_2 doses. Data represent mean ± SD; $n = 3$ independent experiments. *Different to the control in the absence of H_2O_2; $p < 0.05$. #Different to the corresponding parental cells treated with H_2O_2; $p < 0.05$.

50 μM H_2O_2 (Fig. 2B). Mitochondrial depolarization increased significantly in parental cells exposed to 100 or 200 μM H_2O_2. However, mitochondrial function was preserved in Ngb-transfected cells at all the H_2O_2 concentrations investigated.

Changes to intracellular calcium

Prior to treatment with H_2O_2, parental and Ngb-transfected cells showed near identical baseline levels of free Ca^{2+} (Fig. 3). However, a Ca^{2+}-influx was apparent in parental cells exposed to increasing dose of H_2O_2 and this was inhibited by Ngb. Parallel imaging studies with cells overexpressing human Ngb indicated these cells were largely resistant to Ca^{2+}-influx (not shown).

Intracellular ATP

Initially we determined the ratio of ADP/ATP in response to H_2O_2-insult (Fig. 4A).Unaltered ADP/ATP ratios were detected in both parental cells and cells containing the human Ngb–fusion protein when exposed to $H_2O_2 \leq 50\ \mu M$. However, increasing the peroxide challenge to 100 or 200 μM induced a marked increase in the ADP/ATP ratio in parental cells, whereas unexpectedly the ratio decreased below baseline levels in cells transfected with human Ngb. The latter may indicate an increase in ATP or a decrease in the pool of available ADP. To determine whether ATP increased, intracellular ATP was examined independently. Similar to the ADP/ATP ratio, ATP content in parental cells was unaffected by exposure to $\leq 50\ \mu M$ H_2O_2 (Fig. 4B). Thereafter, levels of ATP decreased in a dose-dependent fashion reaching significance at the highest H_2O_2 dose tested. Similarly, Ngb-transfected cells were resistant to 10 or 50 μM H_2O_2. However, ATP increased markedly (~2-fold) in cells transfected with human Ngb following treatment with 100 or 200 μM H_2O_2 (Fig. 4B). Parallel ATP assessment with liquid chromatography confirmed intracellular ATP increased in Ngb overexpressing cells (Figs. 4C and 4D). The lower fold-increase in ATP levels detected by HPLC likely reflects the extraction procedure that may have degraded labile ATP.

Gene regulation

Oxidative stress can elicit an antioxidant gene response in neuronal cells (13, 47). Parental and Ngb-transfected cells

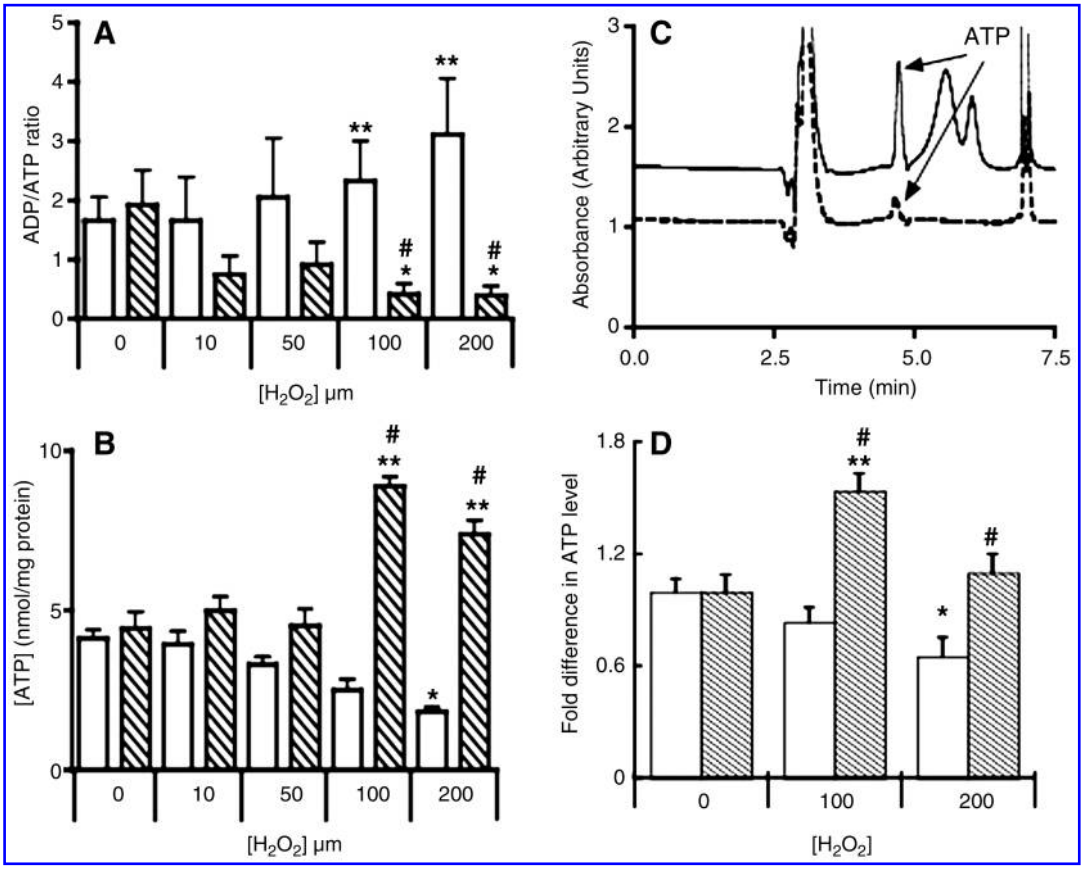

FIG. 4. Changes in cellular energetics in both parental and Ngb-transfected cells following H_2O_2 insult. (**A**) The ratio of ADP/ATP was determined in parental (*open bar*) or Ngb-transfected cells (*hatched bar*) and expressed as mean fluorescent intensity. (**B**) Cellular ATP was measured in parental (*open bar*) and Ngb-transfected cells (*hatched bar*) after exposure to the indicated H_2O_2 dose. (**C**) Changes in cellular ATP reported in (**B**) were corroborated by determining ATP with HPLC as shown for parental (*dashed line*) and Ngb-transfected cells (*filled line*) after exposure to 100 μM H_2O_2. ATP eluted at ~4.8 min (*arrow*) and was verified by spiking with authentic ATP. (**D**) ATP assessed by HPLC was expressed as a fold-change relative to untreated controls (assigned unitary value). In the absence of H_2O_2, ATP concentrations were $\sim 12.1 \pm 1.8$ and $\sim 10.3 \pm 2.1$ nmol/mg cell protein for parental *(open bar)* and Ngb-transfected cells *(hatched bar)*, respectively. Data represent mean ± SD; $n = 4$ independent experiments. *Different to the vehicle-treated control; $p < 0.05$. **Different to the corresponding control; $p < 0.05$. #Different to the corresponding parental cells treated with H_2O_2; $p < 0.05$.

were probed for expression of *HO-1, CAT,* and *MnSOD* as these genes are associated with the stress response (25). Of the genes studied, *HO-1* increased substantially after insult (Fig. 5A and Table 2) and was sustained for up to 12 h (not shown). Cells transfected with human Ngb were resistant to H_2O_2-induced *HO-1* regulation (Table 2).

Parental cells exposed to 200 μM H_2O_2 showed a parallel accumulation of HO-1 protein as demonstrated by Western blot (Fig. 5B). However, no increase in HO-1 protein was detected in Ngb-transfected cells exposed to the same insult. In agreement with the gene and protein studies, total HO activity increased in parental cells when exposed to 100 or 200 μM H_2O_2 (as judged by the extent of bilirubin (BR) accumulation) whereas, HO activity in Ngb-transfected cells was unchanged (Fig. 5C).

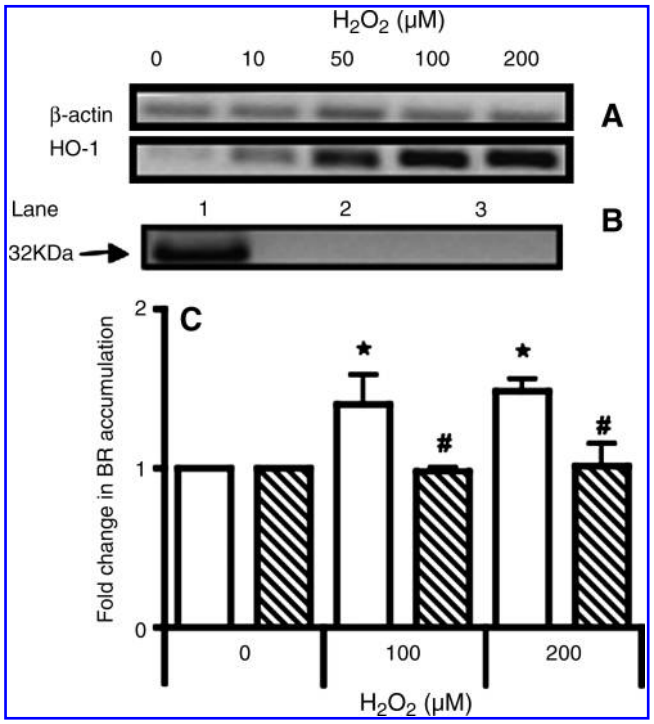

FIG. 5. H_2O_2 regulates gene and protein expression of the early antioxidant response element HO-1. (**A**) Qualitative RT-PCR indicated a H_2O_2-dependent induction of *HO-1* in parental neurons after normalizing to β-actin. (**B**) Microsomes isolated from parental cells showed an increase in HO-1 protein as judged by Western blotting: HO-1 was differentially increased in the presence (*lane 1*) or absence (*lane 2*) of 200 μM H_2O_2. *Lane 3* shows that HO-1 protein was not increased in Ngb-transfected cells treated with 200 μM H_2O_2. (**C**) Induction of *HO-1* is accompanied by increased HO activity in parental (*open bar*), but not Ngb-transfected (*hatched bar*) cells when incubated with 0, 100, and 200 μM H_2O_2. Data represents mean $\pm$ SD; $n = 4$ independent experiments. Changes in HO-1 activity are expressed as a fold-increase relative to vehicle-treated controls (minus H_2O_2) that are arbitrarily assigned a value of 1 (Unit activity corresponds to 5 nmol bilirubin (BR)/mg microsomal protein/min). *Different to the untreated control; $p < 0.05$. #Different to the corresponding parental cells treated with the same H_2O_2 dose; $p < 0.05$.

H_2O_2-mediated changes in receptor-mediated transport and cytoskeletal structure

In the absence of H_2O_2, parental cells and cells overexpressing human Ngb showed similar up-take of fluorescent-labelled transferrin (compare Figs. 6A and 6B). Upon challenge with increasing doses of H_2O_2, parental neurons exhibited a decrease in total fluorescence compared to control and this was more marked for cells exposed to 100 or 200 μM H_2O_2 (compare Figs. 6A and 6C). Under identical experimental conditions, cellular fluorescence remained unchanged in Ngb-transfected cells, indicating that receptor-mediated up-take of labeled transferrin was not altered by H_2O_2 insult (compare Figs. 6B and 6D).

Immuno-staining for the structural protein β-actin indicated little change in the fluorescent distribution for cells exposed to ≤ 50 μM H_2O_2 (not shown). Parental neurons displayed a pattern of condensed actin filaments, particularly along axonal and dendritic processes when challenged with 100 or 200 μM H_2O_2 (compare Figs. 7A and 7C). Reflecting the protective action of human Ngb (Fig. 1), the extent of actin condensation was less evident in Ngb-transfected cells under identical H_2O_2 insult (Figs. 7B and 7D). These data suggest that human Ngb acts to maintain cell membrane integrity and this may assist in maintaining receptor-mediated binding of targeted ligands (Fig. 6).

Assessing the mechanism for Ngb-mediated increase in cellular ATP

The observation that ATP increased in neurons overexpressing human Ngb after 100 or 200 μM H_2O_2 insult (Fig. 4) led to pharmacologic inhibitor studies probing the involvement of the mito-K_{ATP} channel in this process. In the absence of H_2O_2, ATP concentration was $\sim 5.7 \pm 1.6$ nmol/mg cell protein (mean $\pm$ SD; $n = 3$), indicating that treatment with the inhibitors did not alter baseline concentrations of ATP. Treatment of human Ngb overexpressing cells with glybenclamide prior to H_2O_2 insult inhibited the increase H_2O_2-mediated in ATP (Fig. 8A). Phosphorylation of protein within the mito-K_{ATP} channel by PI3K is implicated in

Table 2. Changes to Antioxidant Response Elements in Cultured Neurons after H_2O_2 Insult

	(H_2O_2) (μM)				
Gene	*0*	*10*	*50*	*100*	*200*
Parental cells					
HO-1	1.0 (0.1)	1.2 (0.1)	1.7 (0.1)	2.3 (0.2)	2.5 (0.2)
MnSOD	1.0 (0.1)	1.1 (0.1)	1.2 (0.1)	1.2 (0.1)	1.2 (0.1)
CAT	1.0 (0.1)	1.0 (0.1)	1.1 (0.1)	1.2 (0.1)	1.2 (0.1)
Cells transfected with human Ngb					
HO-1	1.0 (0.1)	1.0 (0.1)	1.0 (0.1)	1.0 (0.1)	1.0 (0.1)
MnSOD	1.0 (0.1)	1.0 (0.1)	1.0 (0.1)	1.0 (0.1)	1.0 (0.1)
CAT	1.0 (0.1)	1.0 (0.1)	1.0 (0.1)	1.0 (0.1)	1.0 (0.1)

Expression of early antioxidant response genes in parental and Ngb-transfected cells were assessed before and after 2 h insult with H_2O_2 (10–200 μM). Data represent mean fold-change relative to vehicle treated controls $\pm$ (SD) from $n = 3$ independent experiments which have been normalized to the corresponding β-actin housekeeping gene.

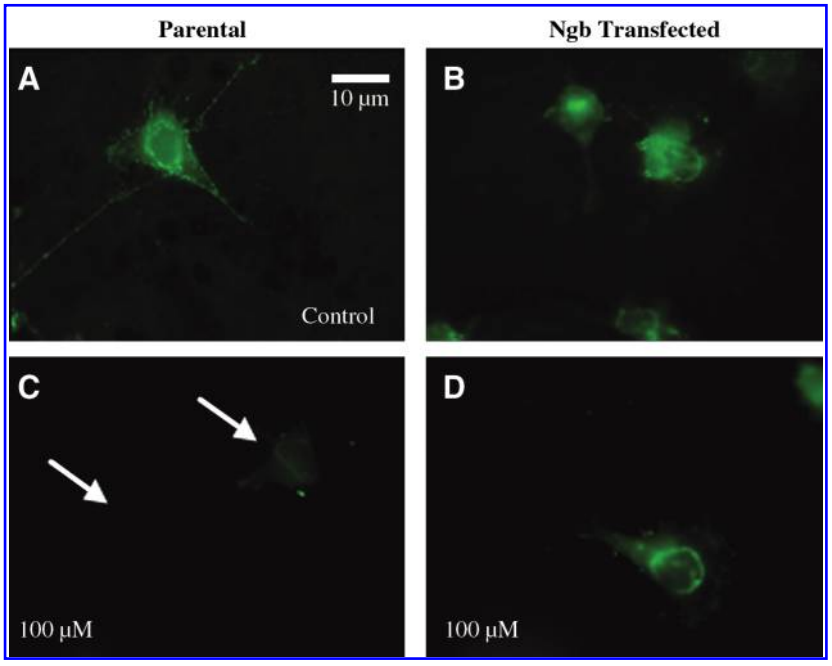

FIG. 6. H_2O_2-stimulates a decrease in transferrin uptake in parental neurons, which is reversed in neurons transfected with human Ngb. Representative micrographs show the distribution of labeled transferrin 15 min after adding the probe and in the absence of H_2O_2. (**A**) vehicle-treated parental cells and (**B**) Ngb-transfected cells. (**C**) Cellular fluorescence is depressed in parental neurons exposed to H_2O_2 (100 μM, 2 h, 37°C) prior to addition of labeled-transferrin (*Arrow* indicates cells with low fluorescence response). (**D**) Ngb-transfected cells show unaltered transferrin uptake following incubation with 100 μM H_2O_2 for 2 h. (For interpretation of the references to color in this figure legend, the reader is referred to the web version of this article at www.liebertonline.com/ars).

regulating the mitochondrial pore (45). Thus, we sought to inhibit PI3K using two structurally unrelated inhibitors (wortmannin and LY294002) to determine the effect on intracellular ATP. Similar to glybenclamide, wortmannin and LY294002 inhibited increases in ATP upon (100 or 200 μM) H_2O_2 insult (Fig. 8A). At least in the case for LY294002, the reversal in ATP accumulation coincided with increased mitochondrial depolarization (Supplemental Fig. 3B), indicating that mitochondrial dysfunction contributed to the ATP loss. Parallel studies on cells pre-incubated with LY294002 showed that cell viability was largely resistant to peroxide insult (Supplemental Fig. 3C). These data indicate an involvement of PI3K in the protective activity of Ngb and that primarily mitochondrial dysfunction contributes to the decreased pool of ATP in Ngb-transfected cells exposed to H_2O_2.

To validate that a PI3K-dependent mechanism was involved in regulating ATP in cells overexpressing Ngb, we monitored total Akt and p-Akt in parental and Ngb-transfected cells before and 2 h after insult with 100 μM H_2O_2 by using Western blotting; we anticipated enhanced Akt phosphorylation (Fig. 8B). In the absence of H_2O_2, total Akt was marginally elevated in Ngb-transfected cells compared to

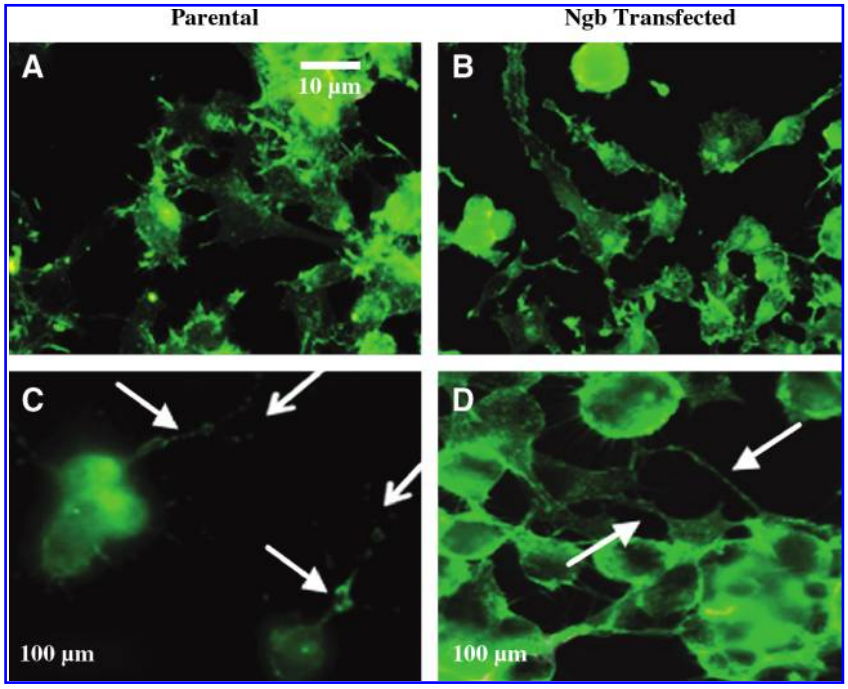

FIG. 7. Condensation of actin filaments in parental cells exposed to H_2O_2 is abrogated by overexpression of human Ngb. Micrographs in panels (**A**) and (**C**) represent parental neuronal cells, while panels (**B**) and (**D**) show Ngb-transfected cells immuno-stained for membranous β-actin using a mouse monoclonal antibody raised against human β-actin. Data shown represent cells before (**A** and **B**) and after (**C** and **D**) incubation (2 h, 37°C) with 100 μM H_2O_2. *Arrows* highlight actin condensation along axonal processes. (For interpretation of the references to color in this figure legend, the reader is referred to the web version of this article at www.liebertonline.com/ars).

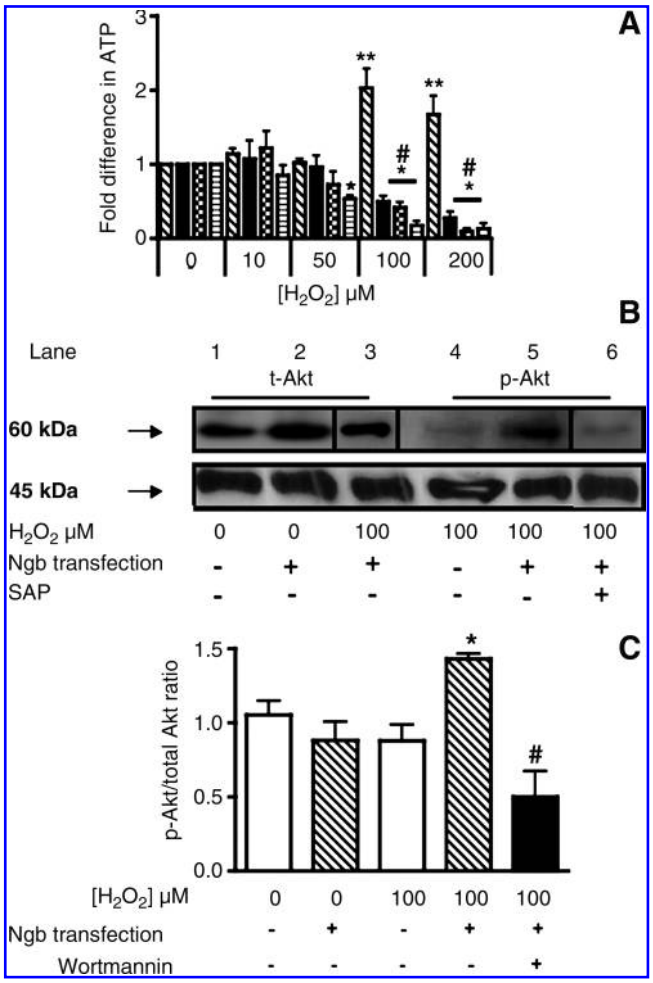

FIG. 8. Enhanced ATP production in Ngb-transfected neurons upon H_2O_2 insult involves opening of the K_{ATP} channel and Akt phosphorylation. (**A**) Ngb-transfected cells were pretreated with glybenclamide (10 μM; *filled bar*), wortmannin (250 n*M*; *checkered bar*), LY294002 (50 μM; *bricked bar*) or vehicle alone (*hatched bar*), then exposed to 0–200 μM H_2O_2, and ATP assessed. Data are expressed as a fold-change relative to control and represent mean ± SD; $n = 9$ independent cell preparations. (**B**) Parental and Ngb-transfected cells were treated with 100 μM H_2O_2 and lysates were assessed for total (t-Akt; ~58 kDa) and phosphorylated Akt (p-Akt; ~60 kDa) by Western blotting. Proteins bands were normalized against β-actin (~ 45 kDa) visualized on a parallel gel. *Lanes 1* and *2*: t-Akt in both parental and Ngb-transfected cells in the absence of H_2O_2 and Shrimp Alkaline Phosphatase (SAP). *Lane 3*: t-Akt in Ngb-transfected cells treated with 100 μM H_2O_2. *Lane 4*: p-Akt in parental cells exposed to 100 μM H_2O_2. *Lane 5*: p-Akt is elevated markedly in Ngb-transfected cells after treatment with 100 μM H_2O_2. *Lane 6*: same as *lane 5* with the exception that 10 μl SAP (1 Unit/μl) was added as a dephosphorylation control. Data are representative of three different cell preparations. (**C**) The ratio of p-Akt/total Akt was determined in parental (*open bar*) or Ngb-transfected cells (*hatched bar*) in the absence or presence of 250 n*M* wortmannin (*black bar*) with a commercial CELISA kit and expressed as a fold-change relative to the corresponding control. Data represent mean ± SD; $n = 6$ cell preparations. *Different to the vehicle-treated control; $p < 0.05$. **Different to the parental cells; $p < 0.05$. #Different to the corresponding Ngb-transfected cells treated at the same H_2O_2 dose; $p < 0.05$.

parental controls while baseline levels of p-Akt remained below the detection limit (not shown). When challenged with 100 μM H_2O_2, a dose that increased intracellular ATP, p-Akt markedly increased in Ngb-transfected cells, while in parental cells p-Akt was detected at lower concentrations under the same conditions. However, total Akt was unchanged in both cell types at these concentrations (not shown). As anticipated, the addition of SAP significantly diminished the level of p-Akt in Ngb-transfected cells exposed to 100 μM H_2O_2 thereby, confirming our assignment of p-Akt to the respective protein bands.

To verify the changes in p-Akt, we next determined the ratio of p-Akt/total Akt under the experimental conditions described above (Fig 8C). In the presence of 100 μM H_2O_2, parental cells showed a marginal decrease in the p-Akt/total Akt ratio. Consistent with the Western blot data, the p-Akt/total Akt ratio ratio increased in cells overexpressing human Ngb and this was inhibited by wortmanin (Fig. 8C).

Pharmacologic activation of PI3K in neuronal cells

To support the idea that Ngb-transfected cells maintained cell viability in response to H_2O_2 challenge via a PI3K dependant pathway, we sought to recapitulate this pathway in parental neurons by administering diazoxide—a selective mito-K_{ATP} channel opener, or leptin—a selective short-term PI3K activator, prior to H_2O_2 insult. Cells pretreated with diazoxide maintained intracellular ATP at all H_2O_2 doses tested, whereas cells exposed to leptin showed an immediate and significant increase in ATP (Fig. 9A) that mimicked that seen in Ngb-transfected cells (Fig. 4).

Parallel assessment of cell viability demonstrated that cells incubated with leptin were highly resistant to necrosis across all H_2O_2 doses, whereas diazoxide-treated cells revealed a trend to lower viability that became significant at the highest H_2O_2 (Fig. 9B). These data indicate that maintenance of the mito-K_{ATP} channel alone is not sufficient to confer protection against necrosis. Notably, pretreatment of parental cells with LY294002 prior to leptin reversed the protective effect of leptin, further reinforcing a role for PI3K in enhancing cell survival in the presence of H_2O_2 insult (Fig. 9B).

Discussion

Parental cells were able to tolerate a relative low level of peroxide insult with functional parameters remaining unchanged at ≤50 μM H_2O_2 challenge likely through the action of endogenous antioxidants. However, cells exposed to H_2O_2 at concentrations greater than 50 μM experienced marked deficits in viability with parallel increases in mitochondrial dysfunction and oxidative stress. Consistent with previous reports (17, 34), overexpression of Ngb inhibited oxidative stress in neuronal cells, thereby supporting the proposition that Ngb acts as a ROS scavenger (37). Cells overexpressing human Ngb also showed decreased mitochondrial dysfunction and Ca^{2+}-influx, muted caspases 3/7 activation, enhanced cell viability, and maintenance of receptor-mediated endocytosis and cytoskeletal integrity.

The ability of Ngb to protect neuronal cells from H_2O_2 challenge through an antioxidant mechanism is established (17) and this may involve preserving mitochondrial function (37). Our data recapitulate the Ngb-mediated protection afforded to mitochondria in neurons exposed to H_2O_2 with a

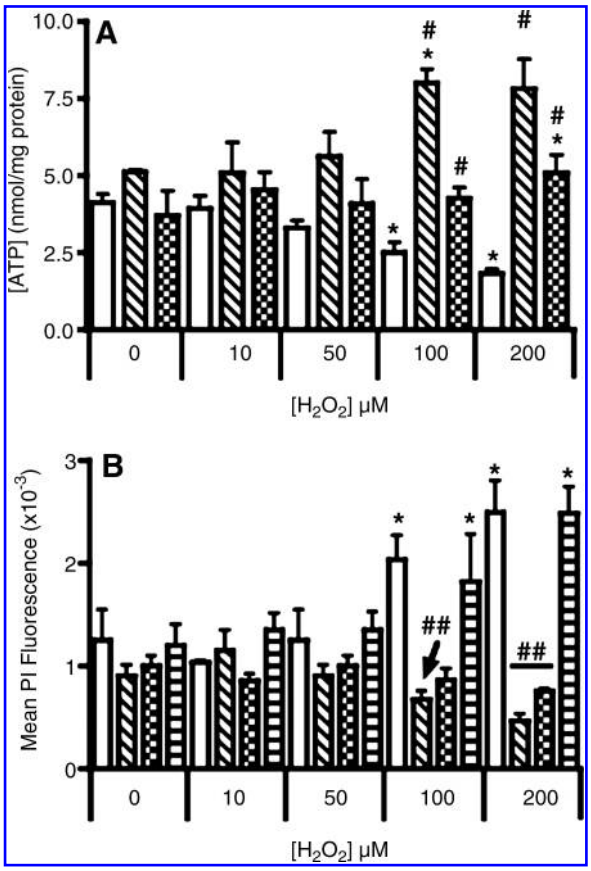

FIG. 9. Cellular ATP increases in parental neurons pre-incubated with leptin or diazoxide. (**A**) ATP content in control cells (*open bar*) or cells pretreated with 100 n*M* leptin (*hatched bar*) or 100 μM diazoxide (*checkered bar*) and exposed to the indicated H_2O_2 dose. (**B**) The extent of propidium iodide (PI) staining in differentiated parental neurons treated with vehicle (*open bar*), 100 n*M* leptin (*hatched bar*), and 100 μM diazoxide (*checkered bar*) was determined by flow cytometry before and after exposure to H_2O_2 for 2 h at the indicated dose. In some experiments, parental cells (*bricked bar*), were co-incubated with 50 μM LY294002 and 100 n*M* leptin prior to H_2O_2 treatment. Data represent mean ± SD; three independent experiments. *Different to the vehicle-treated control in the absence of H_2O_2; $p < 0.05$. #Different to the corresponding parental cells treated with H_2O_2; $p < 0.05$. ##Different to the corresponding control cells pre-incubated with either leptin or diazoxide in the absence of H_2O_2; $p < 0.05$.

consequential decrease in oxidative stress yielding enhanced cell viability. Furthermore, our data demonstrate a H_2O_2-stimulated increase in total ATP within cells overexpressing Ngb. Thus, by preventing an energy deficit (*i.e.*, through increasing the intracellular ATP during oxidative insult), Ngb may also prevent the breakdown of ion homeostasis, release of excitatory neurotransmitters, and excitotoxic stimuli that promote neuronal cell death (6).

Mitochondrial dysfunction leads to the overproduction of $O_2\bullet^-$ that is central to promoting enhanced apoptosis in neuronal cells (58). Maintenance of mitochondrial function may be crucial to cell survival. Therefore, a mechanism whereby Ngb stimulates ATP production during oxidative stress may be critical to maintaining neuronal cell viability and function. Phosphorylated Akt targets to the mitochondria and inhibits the release of apoptosis-inducing factor and cytochrome *c*, thereby inhibiting apoptosis (7, 54). Our results therefore add to the previously identified ROS-scavenging action of Ngb and reveal an involvement for Ngb in peroxide-stimulated PI3K activation and opening of the mito-K_{ATP} channels to preclude apoptotic sequelae associated with acute oxidative stress. Interestingly, the antioxidant catapol inhibits H_2O_2-mediated endothelial cell apoptosis through a mechanism involving activation of the PI3K/Akt signaling pathway (26). Thus consistent with our observations for Ngb in cultured neurons, antioxidants may induce PI3K and preserve cell viability. Alternately, opening of the mito-K_{ATP} channels represents a powerful contributor to neuroprotection (11). Precisely how Ngb is able to modulate PI3K activity and why this activity requires stimulation by added H_2O_2 at doses $>50\,\mu M$ warrants further investigation. Nevertheless, our data reveal that the antioxidant action of Ngb is linked to maintaining cellular energetics and viability during experimental oxidative stress.

Sustained opening of the mito-K_{ATP} channel is associated with cerebral preconditioning against ischemia reperfusion injury (63). Phosphorylation of protein components that comprise the mito-K_{ATP} channel are important in opening of the pore that sustains ATP release. Both PI3K (45) and PKC epsilon (46) are implicated in this regulatory process. In this study, we provide evidence to implicate Ngb in regulating PI3K activity that, in turn, affects the mito-K_{ATP} channel and increases the proportion of p-Akt relative to total Akt. This mode of action for Ngb in the face of challenge with pathological concentrations of H_2O_2 was recapitulated with a pharmacologic activator of PI3K and suggests that Ngb may enhance neuronal cell survival after acute cerebral ischemia, where increased generation of H_2O_2 through uncontrolled production of $O_2\bullet^-$ is implicated (55). Such a link between Ngb and pAkt in neuronal cells may explain the involvement of Ngb in "resetting levels of apoptosis", albeit through mechanisms that do not necessarily involve a direct interaction with cytochrome *c* (8, 15).

How Ngb interacts with H_2O_2 to stimulate PI3K activity is not known. Maintenance of actin cytoskeletal integrity is necessary for PI3K activation (41), however it remains unclear from our data as to whether Ngb-mediated stabilization of actin in turn activates PI3K or whether PI3K is activated directly by Ngb during excessive oxidative stress. In addition, a continuous availability of ATP may underpin PI3K activation. Nevertheless, our studies with leptin or diazoxide show that activation of PI3K and opening of the mito-KATP channel are potentially useful strategies to protect cultured neurons from H_2O_2 insult.

Interestingly, the mito-K_{ATP} channel is reported to be redox sensitive with the oxidation of key proteins involved in pore opening (18). However, ROS activation of the mito-K_{ATP} channel does not seem to be relevant in our experimental system since overexpression of human Ngb downregulated oxidative stress yet enhanced ATP release through the opening the mito-K_{ATP} channel. In addition to redox regulation, *S*-nitrosylation of cysteine residues in the SUR1 subunit activates the mito-K_{ATP} channel (14, 30). Whether human Ngb plays a role in facilitating S-nitrosylation of cysteine residues in the SUR1 subunit is not known and further studies investigating this potential relationship are warranted.

Given the impact of oxidative stress on neuronal function, it was reasonable to consider the expression levels of natural antioxidants, such as HO-1, SOD, and CAT in our cell model (31). The selective induction of HO-1 compared with other antioxidant enzymes has been reported previously (5). Induction of the ARE HO-1 is regulated via transcription factors such as HIF-1α, Nrf2 (29), and AP1 (22), which themselves may be under redox regulation. HO-1 expression is triggered by a variety of stress-inducing stimuli including hypoxia, UV irradiation, H_2O_2, and NO (53). Protective effects of HO-1 are linked to signal transduction and activators of transcription (STAT) proteins (including PI3K) [*e.g.*, STAT3 (64) acting via cytokines IL-6 and IL-10 (12, 34)]. Upstream STAT/JAK signaling is regulated by an influx of Ca^{2+} (40), which is consistent with the observed Ca^{2+}-influx in parental cells exposed to 100 or 200 μM H_2O_2 that corresponded to a induction of HO-1 gene and protein with parallel increases in activity.

The pathological relevance of this study depends on whether neuronal cells are exposed to the H_2O_2 levels used here. Under normal physiological conditions [H_2O_2] is strictly regulated and ranges 0.13–0.25 μM (20). By contrast, [H_2O_2] up to 100 μM are reported in rat striatal tissue following forebrain ischemic injury (28). Furthermore, following cerebral ischemia, infiltrating polymorphonuclear neutrophils (PMN) may be a source of H_2O_2 in affected brain tissues (4). In humans the density of circulating PMN reaches $\sim 1.5\text{-}6\times10^6$ cells/ml. At this cell density 0.08–0.48 mM H_2O_2/h is generated upon exogenous chemical activation (38). Moreover, H_2O_2 is diffusible and less reactive than other ROS; therefore, it is plausible that neurons are exposed (locally) to high micromolar [H_2O_2] in the setting of cerebral ischemia and that H_2O_2-doses of $\sim 100\,\mu M$ may be pathological. Another consideration is the levels of endogenous Ngb versus the 4-fold higher levels achieved through overexpression of the protein here (Supplemental Fig. 1B).

Neuroglobin has been implicated in oxygen transport (44), as an oxygen sensor that initiates the activation of other proteins with regulatory functions (33), or even as a dioxygenase that limits nitrosative stress (59). Though not yet completely understood, Ngb can act to preserve cell viability through multiple protective mechanisms that involve regulation of metal ion homeostasis in neuronal cells (13). The present study expands on these potential activities and links Ngb with the activation of both PI3K and the mito-K_{ATP} channel and an increase in the p-Akt/total Akt ratio in response to an oxidative insult that overwhelms the endogenous antioxidant capacity. Notably, activation of the PI3K/Akt signaling pathway is also implicated in regulating the pro-apoptotic JNK pathway (1). The authors also acknowledge the possibility that H_2O_2 itself may induce Ngb expression (35). However, at least in our hands, no change in the expression of the human Ngb–fusion protein was evident upon H_2O_2 insult (Supplemental Fig. 1A). Studies with Ngb-deficient mice may yield more information on the role for Ngb during cerebral ischemia.

Acknowledgments

This work was supported by the Australian Research Council (DP0343325 and DP0878559) and National Heart Foundation Grants (G07S30435 to PKW and Scholarship PB08S4123 to STA).

Author Disclosure Statement

No competing financial interests exist.

References

1. Aikin R, Maysinger D, and Rosenberg L. Cross-talk between phosphatidylinositol 3-kinase/AKT and c-Jun NH2-terminal kinase mediates survival of isolated human islets. *Endocrinology* 145: 4522–4531, 2004.
2. Allan SM and Rothwell NJ. Cytokines and acute neurodegeneration. *Nat Rev Neurosci* 2: 734–744, 2001.
3. Ardehali H, Chen Z, Ko Y, Mejia–Alvarez R, and Marban E. Multiprotein complex containing succinate dehydrogenase confers mitochondrial ATP-sensitive K+ channel activity. *Proc Natl Acad Sci USA* 101: 11880–11885, 2004.
4. Barone F, Hillegass L, Price W, White R, Lee E, Feuerstein G, Sarau H, Clark R, and Griswold D. Polymorphonuclear leukocyte infiltration into cerebral focal ischemic tissue: myeloperoxidase activity assay and histologic verification. *J Neurosci Res* 29: 336–345, 1991.
5. Barrera D, Maldonado PD, Medina–Campos ON, Hernandez–Pando R, Ibarra–Rubio ME, and Pedraza–Chaverrì J. Protective effect of SnCl2 on K2Cr2O7-induced nephrotoxicity in rats: The indispensability of HO-1 preinduction and lack of association with some antioxidant enzymes. *Life Sci* 73: 3027–3041, 2003.
6. Bickler PE. How brains handle hypoxia: The brain without oxygen: Causes of failure–Physiological and molecular mechanisms for survival. *JEB* 207: 12–13, 2004.
7. Bijur GN and Jope RS,. Rapid accumulation of Akt in mitochondria following phosphatidylinositol 3-kinase activation. *J Neurochem* 87: 1427–1435, 2003.
8. Bonding SH, Henty K, Dingley AJ, and Brittain T. The binding of cytochrome c to neuroglobin: A docking and surface plasmon resonance study. *Int J Biol Macromol* 43: 295–299, 2008.
9. Burmester T and Hankeln T. Neuroglobin: A respiratory protein of the nervous system. *News Physiol Sci* 19: 110–113, 2004.
10. Burmester T, Weich B, Reinhardt S, and Hankeln T. A vertebrate globin expressed in the brain. *Nature* 407: 520–523, 2000.
11. Busija DW, Lacza Z, Rajapakse N, Shimizu K, Kis B, Bari F, Domoki F, and Horiguchi T. Targeting mitochondrial ATP-sensitive potassium channels—A novel approach to neuroprotection. *Brain Res Rev* 46: 282–294, 2004.
12. Deramaudt TB, da silva J–L, Remy P, Kappas A, and Abraham NG. Negative regulation of human heme oxygenase in microvessel endothelial cells by dexamethasone. *Proc Soc Exp Biol Med*. 222: 185–193, 1999.
13. Duong TTH, Witting PK, Antao ST, Parry SN, Kennerson M, Lai B, Vogt S, Lay PA, and Harris HH. Multiple protective activities of neuroglobin in cultured neuronal cells exposed to hypoxia re-oxygenation injury. *J Neurochem* 108: 1143–1154, 2009.
14. Facundo HTF, de Paula JG, and Kowaltowski AJ. Mitochondrial ATP-sensitive K+ channels are redox-sensitive pathways that control reactive oxygen species production. *Free Rad Biol Med* 42: 1039–1048, 2007.
15. Fago A, Mathews AJ, and Brittain T. A role for neuroglobin: Resetting the trigger level for apoptosis in neuronal and retinal cells. *IUBMB Life* 60: 398–401, 2008.
16. Fordel E, Geuens E, Dewilde S, Rottiers P, Carmeliet P, Grooten J, and Moens L. Cytoglobin expression is upregulated in all tissues upon hypoxia: An *in vitro* and *in vivo*

study by quantitative real-time PCR. *Biochem Biophys Res Commun* 319: 342–348, 2004.
17. Fordel E, Thijs L, Martinet W, Lenjou M, Laufs T, Van Bockstaele D, Moens L, and Dewilde S. Neuroglobin and cytoglobin overexpression protects human SH-SY5Y neuroblastoma cells against oxidative stress-induced cell death. *Neurosci Lett* 410: 146–151, 2006.
18. Fornazari M, de Paula JG, Castilho RF, and Kowaltowski AJ. Redox properties of the adenoside triphosphate-sensitive K+ channel in brain mitochondria. *J Neurosci Res* 86: 1548–1556, 2008.
19. Garry DJ and Mammen PPA. Neuroprotection and the role of neuroglobin. *The Lancet* 362: 342–343, 2003.
20. Gonzalez–Flecha B and Demple B. Homeostatic regulation of intracellular hydrogen peroxide concentration in aerobically growing *Escherichia coli. J Bacteriol* 179: 382–388, 1997.
21. Hamdane D, Kiger L, Dewilde S, Green BN, Pesce A, Uzan J, Burmester T, Hankeln T, Bolognesi M, Moens L, and Marden MC. The redox state of the cell regulates the ligand binding affinity of human neuroglobin and cytoglobin. *J Biol Chem* 278: 51713–51721, 2003.
22. Harada H, Sugimoto R, Watanabe A, Taketani S, Okada K, Warabi E, Siow R, Itoh K, Yamamoto M, and Ishii T. Differential roles for Nrf2 and AP-1 in upregulation of HO-1 expression by arsenite in murine embryonic fibroblasts. *Free Rad Res* 42: 297–304, 2008.
23. Harvey J, McKay NG, Walker KS, Van der Kaay J, Downes CP, and Ashford MLJ. Essential role of phosphoinositide 3-kinase in leptin-induced KATP channel activation in the rat CRI-G1 insulinoma cell line. *J Biol Chem* 275: 4660–4669, 2000.
24. Herold S, Fago A, Weber RE, Dewilde S, and Moens L. Reactivity studies of the Fe(III) and Fe(II)NO forms of human neuroglobin reveal a potential role against oxidative stress. *J Biol Chem* 279: 22841–22847, 2004.
25. Hnia K, Hugon G, Rivier F, Masmoudi A, Mercier J, and Mornet D. Modulation of p38 mitogen-activated protein kinase cascade and metalloproteinase activity in diaphragm muscle in response to free radical scavenger administration in dystrophin-deficient Mdx mice. *AMJ Pathol* 170: 633–643, 2007.
26. Hu L, Sun Y, and Hu J. Catalpol inhibits apoptosis in hydrogen peroxide-induced endothelium by activating the PI3K/Akt signaling pathway and modulating expression of Bcl-2 and Bax. *J Euro Pharm* 628: 155–163, 2009.
27. Hundahl C, Kelsen J, Kjaer K, Ronn LCB, Weber RE, Geuens E, Hay–Schmidt A, and Nyengaard JR. Does neuroglobin protect neurons from ischemic insult? A quantitative investigation of neuroglobin expression following transient MCAo in spontaneously hypertensive rats. *Brain Res* 1085: 19–27, 2006.
28. Hyslop PA, Zhang Z, Pearson DV, and Phebus LA. Measurement of striatal H2O2 by microdialysis following global forebrain ischemia and reperfusion in the rat: Correlation with the cytotoxic potential of H2O2 *in vitro. Brain Res* 671: 181–186, 1995.
29. Ishii T, Itoh K, Takahashi S, Sato H, Yanagawa T, Katoh Y, Bannai S, and Yamamoto M. Transcription factor Nrf2 coordinately regulates a group of oxidative stress-inducible genes in macrophages. *J Biol Chem* 275: 16023–16029, 2000.
30. Kawano T, Zoga V, Kimura M, Liang M–Y, Wu H–E, Gemes G, McCallum JB, Kwok W-M, Hogan Q, and Sarantopoulos C. Nitric oxide activates ATP-sensitive potassium channels in mammalian sensory neurons: Action by direct S-nitrosylation. *Mol Pain* 5: 12, 2009.
31. Kinnula VL, Soini Y, Kvist–Makela K, Savolainen E–R, and Koistinen P. Antioxidant defense mechanisms in human neutrophils. *Antiox Redox Signal* 4: 27–34, 2002.
32. Koopman G, Reutelingsperger CP, Kuijten GA, Keehnen RM, Pals ST, and van Oers MH. Annexin V for flow cytometric detection of phosphatidylserine expression on B cells undergoing apoptosis. *Blood* 84: 1415–1420, 1994.
33. Kriegl JM, Bhattacharyya AJ, Nienhaus K, Deng P, Minkow O, and Nienhaus GU. Ligand binding and protein dynamics in neuroglobin. *Proc Natl Acad Sci USA* 99: 7992–7997, 2002.
34. Lee T–S and Chau L–Y. Heme oxygenase-1 mediates the anti-inflammatory effect of interleukin-10 in mice. *Nature Med* 8: 240–246, 2002.
35. Li RC, Morris MW, Lee SK, Pouranfar F, Wang Y, and Gozal D. Neuroglobin protects PC12 cells against oxidative stress. *Brain Res* 1190: 159–166, 2008.
36. Lipton P. Ischemic cell death in brain neurons. *Physiol Rev* 79: 1431–1568, 1999.
37. Liu J, Yu Z, Guo S, Lee S-R, Xing C, Zhang C, Gao Y, Nichools DG, Lo EH, and Wang X. Effects of neuroglobin overexpression on mitochondrial function and oxidative stress following hypoxia/reoxygenation in cultured neurons. *J Neurosci Res* 87: 164–170, 2009.
38. Liu X and Zweier JL. A real-time electrochemical technique for measurement of cellular hydrogen peroxide generation and consumption: Evaluation in human polymorphonuclear leukocytes. *Free Rad Biol Med*. 31: 894–901, 2001.
39. Nilsen IW, ÿverb¯ K, and Olsen RL. Thermolabile alkaline phosphatase from Northern shrimp (*Pandalus borealis*): Protein and cDNA sequence analyses. *CBP Part B: Biochem and Mol Bio* 129: 853–861, 2001.
40. Orellana DI, Quintanilla RA, Gonzalez–Billault C, and Maccioni RB. Role of the JAKs/STATs pathway in the intracellular calcium changes induced by interleukin-6 in hippocampal neurons. *Neurotox Res* 8: 294–304, 2005.
41. Park EH, Kang S–S, Lee Y–S, Kim S–J, Jin E–J, Tak EN, and Sonn JK. Integrity of the cortical actin ring is required for activation of the PI3K/Akt and p38 MAPK signaling pathways in redifferentiation of chondrocytes on chitosan. *Cell Biol Int* 32: 1272–1278, 2008.
42. Park YC, Lee CH, Kang HS, Chung HT, and Kim HD. Wortmannin, a specific inhibitor of phosphatidylinositol-3-kinase, enhances LPS-induced NO production from murine peritoneal macrophages. *Biochem Biophys Res Commun* 240: 692–696, 1997.
43. Peroni D, Negro A, Bähr M, and Dietz GPH. Intracellular delivery of neuroglobin using HIV-1 TAT protein transduction domain fails to protect against oxygen and glucose deprivation. *Neurosci Lett* 421: 110–114, 2007.
44. Pesce A, Dewilde S, Nardini M, Moens L, Ascenzi P, Hankeln T, Burmester T, and Bolognesi M. Human brain neuroglobin structure reveals a distinct mode of controlling oxygen affinity. *Structure* 11: 1087–1095, 2003.
45. Plum L, Ma X, Hampel B, Balthasar N, Coppari R, Münzberg H, Shanabrough M, Burdakov D, Rother E, Janoschek R, Alber J, Belgardt BF, Koch L, Seibler J, Schwenk F, Fekete C, Suzuki A, Mak TW, Krone W, Horvath TL, Ashcroft FM, and Brüning J. Enhanced PIP3 signaling in POMC neurons causes KATP channel activation and leads to diet-sensitive obesity. *J Clin Invest* 116: 1886–1901, 2006.
46. Raval AP, Dave KR, DeFazio RA, and Perez–Pinzon MA. (var epsilon)PKC phosphorylates the mitochondrial K+ ATP

channel during induction of ischemic preconditioning in the rat hippocampus. *Brain Res* 1184: 345–353, 2007.
47. Rayner BS, Duong TTH, Myers SJ, and Witting PK. Protective effect of a synthetic anti-oxidant on neuronal cell apoptosis resulting from experimental hypoxia re-oxygenation injury. *J Neurochem* 97: 211–221, 2006.
48. Sarti C, Rastenyte D, Cepaitis Z, and Tuomilehto J. International trends in mortality from stroke, 1968 to 1994. *Stroke* 31: 1588–1601, 2000.
49. Sidhu JS, Liu F, Boyle SM, and Omiecinski CJ. PI3K inhibitors reverse the suppressive actions of insulin on CYP2E1 expression by activating stress-response pathways in primary rat hepatocytes. *Mol Pharmacol* 59: 1138–1146, 2001.
50. Sims NR and Anderson MF. Mitochondrial contributions to tissue damage in stroke. *Neurochem Int* 40: 511–526, 2002.
51. Sun Y, Jin K, Mao XO, Zhu Y, and Greenberg DA. Neuroglobin is up-regulated by and protects neurons from hypoxic-ischemic injury. *Proc Natl Acad Sci USA* 98: 15306–15311, 2001.
52. Sun Y, Jin K, Peel A, Mao XO, Xie L, and Greenberg DA. Neuroglobin protects the brain from experimental stroke *in vivo*. *Proc Natl Acad Sci USA* 100: 3497–3500, 2003.
53. Tanaka S, Akaike T, Fang J, Beppu T, Ogawa M, Tamura F, Miyamoto Y, and Maeda H. Antiapoptotic effect of haem oxygenase-1 induced by nitric oxide in experimental solid tumour. *Br J Cancer* 88: 902–909, 2003.
54. Tapodi A, Debreceni B, Hanto K, Bognar Z, Wittmann I, Gallyas F Jr, Varbiro G, and Sumegi B. Pivotal role of Akt activation in mitochondrial protection and cell survival by poly(ADP-ribose)polymerase-1 inhibition in oxidative stress. *J Biol Chem* 280: 35767–35775, 2005.
55. Thomas SR, Witting PK, and Drummond GR. Redox control of endothelial function and dysfunction: Molecular mechanisms and therapeutic opportunities. *Antiox Redox Signal* 10: 1713–1766, 2008.
56. Wakasugi K and Morishima I. Identification of residues in human neuroglobin crucial for guanine nucleotide dissociation inhibitor activity 2020. *Biochemistry* 44: 2943–2948, 2005.
57. Wang S, Cone J, and Liu Y. Dual roles of mitochondrial KATP channels in diazoxide-mediated protection in isolated rabbit hearts. *AJP Heart Circ Physiol* 280: H246–255, 2001.
58. Weber T, Dalen H, Andera L, Negre–Salvayre A, Auge N, Sticha M, Lloret A, Terman A, Witting PK, Higuchi M, Plasilova M, Zivny J, Gellert N, Weber C, and Neuzil J. Mitochondria play a central role in apoptosis induced by B1-tocopheryl succinate, an agent with antineoplastic activity; Comparison with receptor-mediated pro-apoptotic signaling. *Biochemistry* 42: 4277–4291, 2003.
59. Witting PK, Douglas DJ, and Mauk AG. Reaction of human myoglobin and nitric oxide. Heme iron or protein sulfhydryl (S) nitrosation dependence on the absence or presence of oxygen. *J Biol Chem* 276: 3991–3998, 2001.
60. Witting PK, Harris HH, Rayner BS, Aitken JB, Dillon CT, Stocker R, Lai B, Cai Z, and Lay PA. The endothelium-derived hyperpolarizing factor, H2O2, promotes metal-ion efflux in aortic endothelial cells: Elemental mapping by a hard X-ray microprobe. *Biochemistry* 45: 12500–12509, 2006.
61. Wynants J and Van Belle H. Single-run high-performance liquid chromatography of nucleotides, nucleosides, and major purine bases and its application to different tissue extracts. *Anal Biochem* 144: 258–266, 1985.
62. Wystub S, Laufs T, Schmidt M, Burmester T, Maas U, Saaler–Reinhardt S, Hankeln T, and Reuss S. Localization of neuroglobin protein in the mouse brain. *Neurosci Lett* 346: 114–116, 2003.
63. Yamada K and Inagaki N. Neuroprotection by KATP channels. *J Mol Cell Cardiol* 38: 945–949, 2005.
64. Zhang X, Shan P, Jiang G, Zhang SSM, Otterbein LE, Fu X–Y, and Lee PJ. Endothelial STAT3 is essential for the protective effects of HO-1 in oxidant-induced lung injury. *FASEB J* 20: 2156–2158, 2006.
65. Zivin JA. Clinical trials of neuroprotective therapies. *Stroke* 38: 791–793, 2007.

Address correspondence to:
Dr. Paul Witting
Redox Biology Group
Discipline of Pathology
Bosch Institute
The University of Sydney
Sydney NSW 2006
Australia

E-mail: pwitting@med.usyd.edu.au

Date of first submission to ARS Central, November 3, 2009; date of final revised submission, March 24, 2010; date of acceptance, April 1, 2010.

Abbreviations Used

Akt = serine/threonine-specific protein kinase
ARE = antioxidant response element
BR = bilirubin
CAT = catalase
DHR-123 = dihydrorhodamine-123
H_2O_2 = hydrogen peroxide
HO-1 = inducible hemoxygenase-1
HPSS = HEPES-buffered physiological saline solution
Ngb = neuroglobin
$O_2^{\bullet -}$ = superoxide anion radical
p-Akt = phosphorylated serine/threonine-specific protein kinase
PBS = phosphate buffered saline
PI3K = phosphatidyl-inositol-3-kinase
ROS = reactive oxygen species
SAP = shrimp alkaline phosphatase
SOD = superoxide dismutase

This article has been cited by:

1. Christophe Lechauve, Sébastien Augustin, Hélène Cwerman-Thibault, Aïcha Bouaita, Valérie Forster, Chantal Célier, Pierre Rustin, Michael C. Marden, José-Alain Sahel, Marisol Corral-Debrinski. 2012. Neuroglobin involvement in respiratory chain function and retinal ganglion cell integrity. *Biochimica et Biophysica Acta (BBA) - Molecular Cell Research* . [CrossRef]
2. Jing Wang, Wei Zhang, Dianjun Sun, Li Song, Yuanyuan Li, Chunbei Xu. 2012. Analysis of neuroglobin mRNA expression in rat brain due to arsenite-induced oxidative stress. *Environmental Toxicology* **27**:9, 503-509. [CrossRef]
3. José Pablo Vázquez-Medina, Tania Zenteno-Savín, Robert Elsner, Rudy M. Ortiz. 2012. Coping with physiological oxidative stress: a review of antioxidant strategies in seals. *Journal of Comparative Physiology B* **182**:6, 741-750. [CrossRef]
4. Donald Wlodkowic. 2012. The case for multiparameter cytometry in neurobiology. *Cytometry Part A* **81A**:7, 544-545. [CrossRef]
5. J. Skommer, S. Helbo, K. Henty, T. Brittain. 2012. Ligand binding, reactivity and biological activity of a distal pocket mutant of neuroglobin. *International Journal of Biological Macromolecules* . [CrossRef]
6. Heung Man Lee, George H. Greeley, Ella W. Englander. 2011. Transgenic overexpression of neuroglobin attenuates formation of smoke-inhalation-induced oxidative DNA damage, in vivo, in the mouse brain. *Free Radical Biology and Medicine* . [CrossRef]
7. Gunnar P.H. Dietz. 2011. Protection by neuroglobin and cell-penetrating peptide-mediated delivery in vivo: A decade of research. *Experimental Neurology* . [CrossRef]
8. Li-Ming Chen, Yan-Si Xiong, Fan-Li Kong, Min Qu, Qun Wang, Xiao-Qian Chen, Jian-Zhi Wang, Ling-Qiang Zhu. 2011. Neuroglobin attenuates Alzheimer-like tau hyperphosphorylation by activating Akt signaling. *Journal of Neurochemistry* no-no. [CrossRef]
9. Elisabetta De Marinis, Maria Marino, Paolo Ascenzi. 2011. Neuroglobin, estrogens, and neuroprotection. *IUBMB Life* **63**:3, 140-145. [CrossRef]
10. Weiguang Li, Yonghong Wu, Changhong Ren, Yiming Lu, Yan Gao, Xiaofei Zheng, Chenggang Zhang. 2011. The activity of recombinant human neuroglobin as an antioxidant and free radical scavenger. *Proteins: Structure, Function, and Bioinformatics* **79**:1, 115-125. [CrossRef]
11. Thomas Brittain, Joanna Skommer, Kristen Henty, Nigel Birch, Subhadip Raychaudhuri. 2010. A role for human neuroglobin in apoptosis. *IUBMB Life* **62**:12, 878-885. [CrossRef]
12. Elisabetta De Marinis, Paolo Ascenzi, Marco Pellegrini, Paola Galluzzo, Pamela Bulzomi, Maria Angeles Arevalo, Luis Miguel Garcia-Segura, Maria Marino. 2010. 17#-Estradiol – A New Modulator of Neuroglobin Levels in Neurons: Role in Neuroprotection against H₂O₂-Induced Toxicity. *Neurosignals* **18**:4, 223-235. [CrossRef]